Research Paper https://doi.org/10.7733/jnfcwt.2020.18.2.169

Corrosion Behavior of Stainless Steel 316 for Carbon Anode Oxide Reduction Application

Min Ku Jeon[1,2,*], Sung-Wook Kim[1], and Eun-Young Choi[1,2]
[1]*Korea Atomic Energy Research Institute, 111, Daedeok-daero 989beon-gil, Yuseong-gu, Daejeon, Republic of Korea*
[2]*University of Science and Technology, 217, Gajeong-ro, Yuseong-gu, Daejeon, Republic of Korea*

(Received January 29, 2020 / Revised May 11, 2020 / Approved June 11, 2020)

Here, the stability of stainless steel 316 (SS-316) was investigated to identify its applicability in the oxide reduction process, as a component in related equipment, to produce a complicated gas mixture composed of O_2 and Cl_2 under an argon (Ar) atmosphere. The effects of the mixed gas composition were investigated at flow rates of 30 mL/min O_2, 20 mL/min O_2 + 10 mL/min Cl_2, 10 mL/min O_2 + 20 mL/min Cl_2, and 30 mL/min Cl_2, each at 600℃, during a constant argon flow rate of 170 mL/min. It was found that the corrosion of SS-316 by the chlorine gas was suppressed by the presence of oxygen, while the reaction proceeded linearly with the reaction time regardless of gas composition. Surface observation results revealed an uneven surface with circular pits in the samples that were fed mixed gases. Thermodynamic calculations proposed the combination of Fe and Ni chlorination reactions as an explanation for this pit formation phenomenon. An exponential increase in the corrosion rate was observed with an increase in the reaction temperature in a range of 300 ~ 600℃ under a flow of 30 mL/min Cl_2 + 170 mL/min Ar.

Keywords: Stainless steel 316, Chlorine, Oxygen-chlorine mixed gas, Oxide reduction, Pyroprocessing

*Corresponding Author.
Min Ku Jeon, Korea Atomic Energy Research Institute, E-mail: minku@kaeri.re.kr, Tel: +82-42-868-2435

ORCID
Min Ku Jeon http://orcid.org/0000-0001-8115-3241
Sung-Wook Kim http://orcid.org/0000-0002-5537-4793
Eun-Young Choi http://orcid.org/0000-0003-1693-7642

1. Introduction

During the operation of 20 pressurized water reactors (PWRs), 300 tons of PWR used nuclear fuel (UNF) are produced every year in Korea. The absence of repository for UNF leaves no choice but to store it in wet storage systems located at the reactor sites. The Korean government is considering options for UNF management, including the recycling of the UNF using pyroprocessing-sodium fast reactor (SFR) technology [1-2]. The role of pyroprocessing in this concept is to supply U and transuranic (TRU) nuclides as a fuel for the SFR via a treatment of the PWR UNF. It was demonstrated by the Argonne National Laboratory in the USA that pyroprocessing technology is feasible for use with a metal fuel recycle system in the Experimental Breeder Reactor-II (EBR-II) system, a type of SFR [3]. Unfortunately, this metal fuel pyroprocessing technique is not directly applicable to the Korean case, as the starting material, PWR UNF, exists in the form of a UO_2 based oxide. To address this, an oxide reduction (OR) process was proposed to convert the oxide fuel into a metallic form. This topic has been the subject of intensive research by various research groups [4-8].

The conventional OR process employs an electrochemical reaction using Li_2O (~1 wt%) incorporated LiCl salt, where Li_2O is electrochemically decomposed into Li metal (at cathode) and oxygen gas (at anode). Operational temperature of the OR process is normally set at 650℃, which is slighltly higher than its melting point, 610℃. The Li metal generated at the cathode electrode of the OR system reacts with UNF oxides to produce Li_2O and metallic UNF. This scheme enables the in-system recycling of Li_2O and Li to keep the concentration of Li_2O in the salt constant. The OR process normally employs platinum as the anode electrode material; however, the high cost and low potential limit of this approach have been pointed out as a bottleneck for large systems. As an alternative to Pt, an OR process operating at a high potential based on a carbon anode was proposed recently [9-10]. In order to achieve high throughput of the system, this high-potential carbon-anode system applies high potential (above 5 V) to a level high enough to decompose the LiCl salt itself. Although this high-potential carbon-anode concept changed the source of Li from Li_2O to LiCl, the LiCl salt still contains Li_2O as a reaction product between Li and oxides in UNF (e.g., $UO_2 + 4Li \rightarrow U + 2Li_2O$). Oxygen ions of Li_2O electrochemically migrates towards anode electrode to produce not only oxygen gas but also CO and CO_2 by reacting with the carbon-anode electrode. As a result, Cl_2, O_2, CO, and CO_2 gases are generated at the carbon-anode electrode under an argon atmosphere during an operation of the high-potential OR process. This condition is new to the field of equipment design, as oxygen had been the only gaseous product at the Pt anode electrode.

Chlorine gas is well-known for its highly corrosive characteristics, and the high operating temperature of the OR process may accelerate the corrosion process. Brown and co-workers [11] conducted extensive corrosion experiments for various commercial alloys under a chlorine or

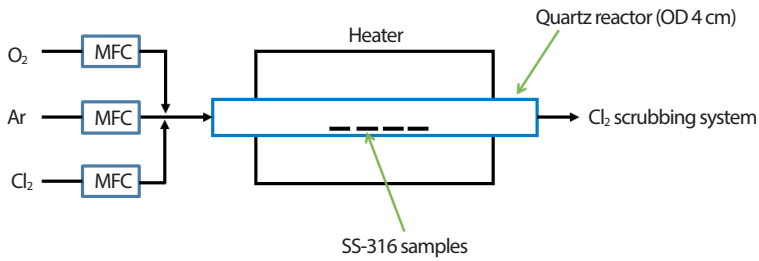

Fig. 1. Schematic diagram of the experimental set-up employing three mass flow controllers (MFCs) for each O_2, Ar, and Cl_2 gas, and a horizontal quartz tube as an inert reactor under a mixed O_2/Cl_2 atmosphere.

hydrogen chloride atmosphere. In this work, the suggested upper temperature limit for continuous service for carbon steel under a dry chlorine atmosphere was 204℃. Nickel and nickel-based alloys such as Inconel and Hastelloy could be employed up to 538℃. Ihara and co-workers [12] reported that the addition of oxygen to hydrogen chloride gas has accelerated corrosion of iron. However, fundamental information to refer in the design of an OR equipment is unavailable especially for oxygen-chlorine mixed gas conditions. In this study, the corrosion reaction of stainless steel 316 (SS-316) by a mixed gas of oxygen and chlorine was investigated under various conditions in an effort to provide fundamental information pertaining the design of equipment for use in the OR process based on carbon anodes. The effects of CO and CO_2 were not considered in this work, which will be a future research subject.

2. Experimental

A horizontal quartz reactor was employed for the reaction experiments as shown in Fig. 1. SS-316 samples (Nilaco, Japan) were cut into 30 mm × 10 mm pieces (1.03 mm thickness) and thoroughly washed using deionized (DI) water and ethanol before the experiments. Four pieces were used for each experiment with weights in the approximate range of 8.5 ~ 9.5 g. The feed gas composition was controlled using mass flow controllers for each gas (argon, chlorine, oxygen).

The effects of the gas composition were investigated at 600℃ for various feed gas compositions of 30 mL/min Cl_2, 20 mL/min Cl_2 + 10 mL/min O_2, 10 mL/min Cl_2 + 20 mL/min O_2, and 30 mL/min O_2 while keeping the flow rate of Ar at 170 mL/min. The progress of corrosion reaction as a function of time at each gas composition was studied by repeating identical experiments for various durations of 1, 2, 4, and 8 h. An additional experiment was conducted at 600℃ by flowing 20 mL/min Cl_2 + 180 mL/min Ar in an effort to identify the effect of oxygen. After each reaction is finished, the samples were washed using DI water and ethanol in order to remove chloride or fragmented oxide scales remaining on surface of the samples.

The HSC chemistry software (version 9.5.1) was employed for thermodynamic calculations [11]. HSC stands for enthalpy (H), entropy (S), and heat capacity (C_p), as it was designed for various chemical reactions and equilibrium calculations based on thermodynamic values. Thermodynamic values of reaction equations were derived using the "Reaction Equations" module. A stable oxide form of Fe under the experimental condition was determined using the "Phase Stability Diagram" module. The formation of chlorides and oxides as a function of Cl_2-O_2 input amount was investigated using the "Equilibrium Compositions" module. In this calculation, initial amount of each metal was fixed as 0.71 moles for Fe, 0.12 moles for Ni, and 0.17 moles for Cr and then 0.2 mol Cl_2 + 0.2 mol O_2 were mixed at 600℃ to calculate the composition at an equilibrium state. The calculations were repeated ten times by adding 0.2 moles of Cl_2 and 0.2 moles of O_2 in each step. The chloride/oxide ratio was calculated using the equilibrium composition results of each step.

The effects of the temperature on the reaction between SS-316 and chlorine gas were investigated under an argon-chlorine atmosphere. These experiments were conducted at various temperatures, in this case 300, 400, 500, and 600℃, while holding the feed gas composition at 30 mL/min Cl_2 + 170 mL/min Ar for 8 h.

The morphologies of the samples after the reactions were investigated using scanning electron microscopy (SEM, Hitachi SU-8020) with energy dispersive X-ray spectroscopy (EDS, Horiba, X-MAX) for a composition analysis. The specimens were thoroughly washed before the surface observation experiments to remove surface scales, as the scales reacted with water vapor as soon as the specimens were exposed to the air after corrosion experiments. The surface and composition analysis experiments were conducted for these washed surfaces ("After washing" in Fig. 2).

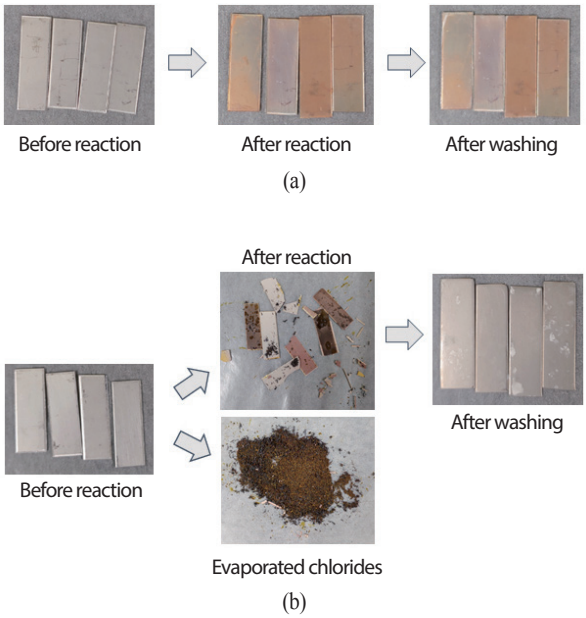

Fig. 2. Images of SS-316 samples before and after the reaction at 600℃ for 8 h at flow rates of 170 mL/min for Ar with (a) 30 mL/min for O_2 or (b) 30 mL/min Cl_2. Images after washing by DI water and ethanol are also shown.

3. Results and Discussion

Fig. 2 shows images of two samples (treated in O_2 and Cl_2 atmosphere, respectively) before and after the reaction at 600℃, and after thorough washing with DI water and ethanol. The reaction temperature was set to the maximum temperature that a component of OR equipment might be exposed. The OR process normally keeps the temperature of LiCl salt at 650℃, and lower parts of electrodes are immersed in the salt. Except the immersed parts of the electrodes, the other parts are located over the salt level where the temperature is lower than 650℃. When oxygen was employed without chlorine (Fig. 2(a)), slight changes in the weight were observed with color changes by forming surface oxide layer. However, the weight change was less than 0.1wt% in all cases when chlorine was absent. When chlorine was utilized in the reaction, profound changes were observed, as shown in Fig. 2(b). First, significant amounts of evaporated reaction products (metal chlorides) were collected at the end point of the quartz reactor as shown in Fig. 2(b) (evaporated chlorides). Second, gray-brown color residue was observed on the samples (see "After reaction" in Fig. 2(b)). The residue was easily broken and separated while discharging the samples from the quartz reactor, and it was completely washed away during the washing step, as shown in the figure ("After washing"). It should be noted that these reaction products with chlorine began to absorb water immediately when exposed to air, which is a common behavior of metal chlorides. Here, physical properties of chlorides of major components (Fe, Ni, and Cr) are helpful in understanding the separation of reaction products into evaporated and residual ones. It is well known that $FeCl_3$ is a volatile compound having a boiling point of 316℃, and expected as the major constituent of the evaporated products. On the other hand, $NiCl_2$ and $CrCl_3$ are expected to remain as residues according to previously reported volatilization on-set temperature of $NiCl_2$ (653℃) [14] and high boiling point (1300℃) of $CrCl_3$.

The effects of the mixed gas conditions are summarized in Fig. 3. As noted in the experimental section, the composition of the mixed gas was set to have an overall flow rate of 30 mL/min with a fixed argon flow rate of 170 mL/min. Thus, four cases of 30 mL/min Cl_2, 20 mL/min Cl_2 + 10 mL/min O_2, 10 mL/min Cl_2 + 20 mL/min O_2, and 30 mL/min O_2 were employed in this work. In all cases, linear relationships between the reaction time and weight loss were observed, as shown in Fig. 3(a). The slope of the linear fitting results increased from 0 to 0.84, 2.0, and to 5.6 with an increase in the Cl_2 flow rate, as shown in the figure. It should be noted that the slopes of the linear fitting results are not proportional to the flow rate of Cl_2. Corrosion rate as a function of chlorine flow rate is shown in Fig. 3(b), and a linear fitting was observed in a logarithm scale meaning that adding oxygen leads to reduced corrosion rate. A comparison experiment was conducted under the condition of 20 mL/min Cl_2 + 180 mL/min Ar for 4 h and the resulting corrosion rate was 1.74×10^2 g/m^2·h, which was 150% higher than the 20 mL/min Cl_2 + 10 mL/min O_2 + 170 mL/min

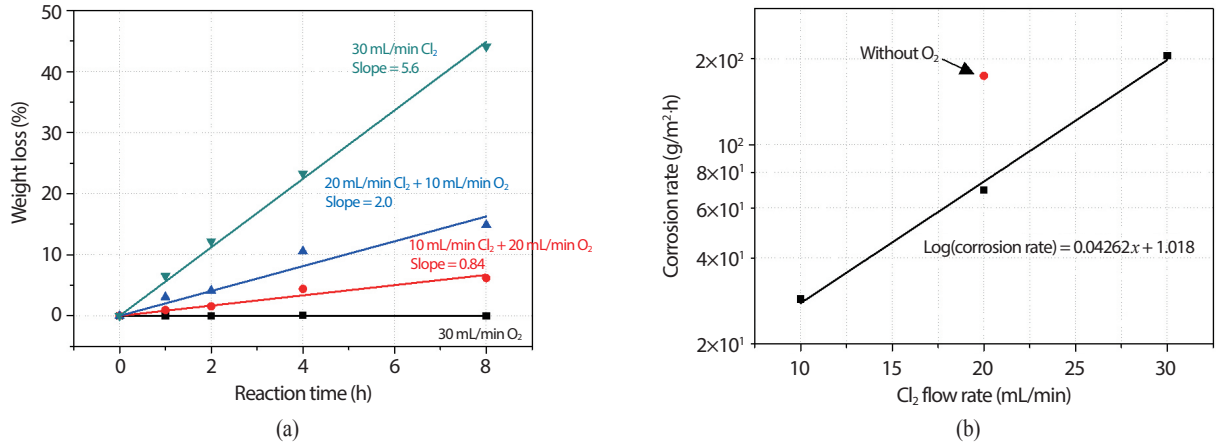

Fig. 3. (a) The effect of the reaction time on weight loss for various gas compositions at 600℃.
(b) The effect of the chlorine flow rate on the corrosion rate at 600℃. Fitting results are also shown as a solid curve.
The data obtained at a flow rate of 180 mL/min Ar + 20 mL/min Cl_2 is denoted as the "Without O_2" case.

Ar case. These results clarify that oxygen acts as an inhibitor in the reaction between SS-316 and the chlorine gas. The suppressing role of oxygen is quite different from the previous report, which claimed accelerated corrosion of iron by adding oxygen to hydrogen chloride [12]. The reaction equations shown below were proposed as the reaction pathways that rationalize the accelerated corrosion by oxygen addition.

$$Fe + 2\,HCl(g) + 1/2\,O_2(g) \rightarrow FeCl_2 + H_2O(g)$$
$$(\Delta G = -231.4\ \text{kJ},\ K = 7.01\times10^{13}\ \text{at}\ 600℃) \quad (1)$$

$$FeCl_2 + HCl(g) + 1/4\,O_2(g) \rightarrow FeCl_3(g) + 1/2\,H_2O(g)$$
$$(\Delta G = -4.549\ \text{kJ},\ K = 1.87\ \text{at}\ 600℃) \quad (2)$$

The negative Gibbs free energy change (ΔG) values and equilibrium constants (K) larger than 1.0 suggests that the above reactions might proceed to the right-hand direction. However, the experimental results of the present work clarify that the above accelerating mechanism does not fit in the corrosion reaction of SS-316 under a Cl_2-O_2 mixed atmosphere. The suppressing effect of oxygen brought about a question: what will occur if SS-316 samples are pre-oxidized instead of feeding a mixed gas? An experiment was conducted to verify the effect of pre-oxidation by flowing 20 mL/min of oxygen for 4 h at 600℃, with the gas then replaced by chlorine at an identical flow rate for 4 h while an argon flow of 180 mL/min was kept constant through the entire reaction procedure. This experiment resulted in a corrosion rate of 1.67×10^2 g/m^2·h, which is close to the value of 1.74×10^2 g/m^2·h in the 20 mL/min Cl_2 case. This outcome reveals that the pre-oxidation process failed to produce a chlorine-resistant oxide film on the surface of SS-316.

One factor that attracted the attention of the authors was the surface morphology of the samples, especially when a comingled gas was employed. Fig. 4 shows photographs of the washed samples reacted at 600℃ for 4 h under different gas conditions. When only oxygen was fed, a smooth surface was observed in both the digital camera images and the SEM images. In the chlorine-only case, the samples lost their shiny surface owing to a severe reaction with chlorine gas, resulting in a relatively rough surface, as shown in the SEM image. Very interesting outcomes from this experiment arose when the mixed gas was introduced. Circular pits were observed in the digital camera images of the 20 mL/min O_2 + 10 mL/min Cl_2 and 10 mL/min O_2 + 20 mL/min Cl_2 samples. An SEM image of the 20 mL/min

Digital camera pictures

30 mL/min O_2 | 20 mL/min O_2 + 10 mL/min Cl_2 | 10 mL/min O_2 + 20 mL/min Cl_2 | 30 mL/min Cl_2

SEM images

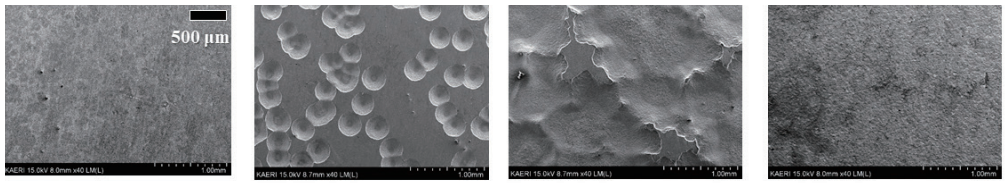

30 mL/min O_2 | 20 mL/min O_2 + 10 mL/min Cl_2 | 10 mL/min O_2 + 20 mL/min Cl_2 | 30 mL/min Cl_2

Fig. 4. Digital camera images and SEM images after the reaction with various gas compositions at 600℃ for 4 h followed by thorough washing.

Table 1. EDS analysis results of the SS-316 samples before and after the reaction with various gas compositions at 600℃ for 4 h. Only major components, Fe, Cr, and Ni, are counted for comparison

	Fe (wt%)	Cr (wt%)	Ni (wt%)	Cr/Ni ratio
Bare SS-316	72.26	17.58	10.17	1.73
30 mL/min O_2	71.28	17.4	11.34	1.54
20 mL/min O_2 + 10 mL/min Cl_2 (smooth)	73.07	16.54	10.41	1.59
20 mL/min O_2 + 10 mL/min Cl_2 (pit)	72.14	18.97	8.90	2.14
10 mL/min O_2 + 20 mL/min Cl_2 (smooth)	70.75	18.19	11.08	1.65
10 mL/min O_2 + 20 mL/min Cl_2 (pit)	71.64	19.93	8.44	2.37
30 mL/min Cl_2	71.15	18.19	10.67	1.71

Table 2. List of reaction equations of metals and oxides of Fe, Cr, and Ni with chlorine at 600℃. The Gibbs free energy change and equilibrium constant values were calculated using the HSC chemistry software

Reaction	ΔG (kJ)	K
$Fe + Cl_2(g) \rightarrow FeCl_2$	-231.8	7.37×10^{13}
$Fe + 3/2\ Cl_2(g) \rightarrow FeCl_3(g)$	-236.5	1.41×10^{14}
$Fe_2O_3 + 3\ Cl_2(g) \rightarrow 2\ FeCl_3(g) + 3/2\ O_2(g)$	119.5	7.07×10^{-8}
$Cr + 3/2\ Cl_2(g) \rightarrow CrCl_3$	-346.0	5.01×10^{20}
$Cr_2O_3 + 3\ Cl_2(g) \rightarrow 2\ CrCl_3 + 3/2\ O_2(g)$	215.6	1.27×10^{-13}
$Ni + Cl_2(g) \rightarrow NiCl_2$	-173.9	2.55×10^{10}
$NiO + Cl_2(g) \rightarrow NiCl_2 + 1/2\ O_2(g)$	-14.29	7.16×10^{0}

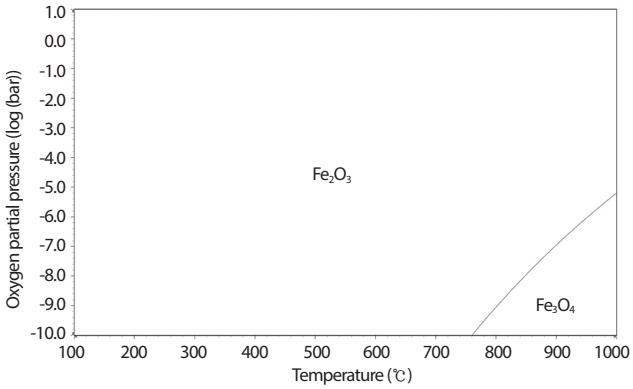

Fig. 5. Phase stability diagram of Fe-O-Ar derived using the HSC chemistry code.

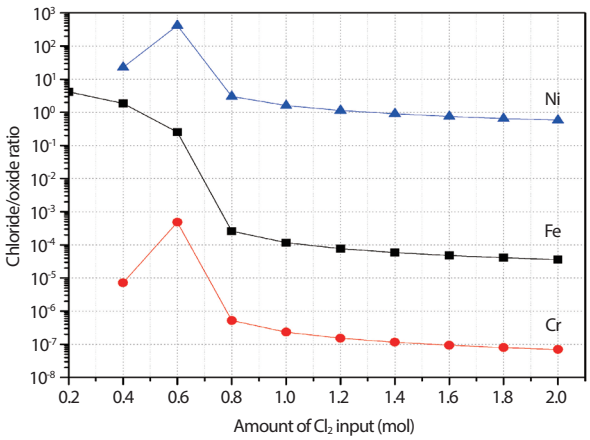

Fig. 6. The chloride/oxide ratio calculation results as a function of amount of Cl_2 input at 600℃. Oxygen of identical amount to that of Cl_2 was also included in the calculations. Initial input amount of each metal is 0.71 moles for Fe, 0.12 moles for Ni, and 0.17 moles for Cr.

O_2 + 10 mL/min Cl_2 sample clearly indicates the formation of circular pits. In the experiment with 10 mL/min O_2 + 20 mL/min Cl_2, the circular pits grew considerably to leave smooth unreacted islands at some locations. These results suggest that the presence of oxygen leads to an uneven reaction on the SS-316 surface, which is presumably the key role of oxygen in suppressing the reaction between SS-316 and chlorine gas. A composition analysis was conducted with bare SS-316 sample and the samples shown in Fig. 4. These results are presented in Table 1. In the 20 mL/min O_2 + 10 mL/min Cl_2 and 10 mL/min O_2 + 20 mL/min Cl_2 cases, the analyses were performed independently for the smooth surfaces and pit locations. The table also includes the Cr/Ni ratio values for comparison purposes, as the composition of iron did not significantly change with the reaction condition. The most significant change in the Cr/Ni ratio was that the values became meaningfully high in the pits of the 20 mL/min O_2 + 10 mL/min Cl_2 and 10 mL/min O_2 + 20 mL/min Cl_2 samples. On the other hand, the Cr/Ni ratio values were slightly lower at the smooth surfaces of mixed gas samples. It was also interesting to find that the lowest Cr/Ni ratio was observed in the 30 mL/min O_2 case, while the composition in the 30 mL/min Cl_2 case is nearly identical to that of the bare SS-316.

Here, HSC chemistry code [11] was employed in order to understand the effect of oxygen addition via thermodynamic basis. The reactions of metals and oxides of Fe, Cr, and Ni with chlorine are listed in Table 2 with the ΔG and K values at 600℃. Clearly, the three major metals are expected to react with chlorine gas spontaneously according to the ΔG (negative) and K (larger than 1.0) values. Before the calculation for oxides, oxidation status of Fe had to be determined as it has various oxide forms such as FeO, Fe_2O_3, and Fe_3O_4. Fig. 5 shows the phase stability diagram derived using the HSC chemistry code, and it is obvious that Fe_2O_3 might be the reaction product at the condition of this study. According to Table 2, NiO is reactive with chlorine gas, while Fe_2O_3 and Cr_2O_3 are not. The conversion of NiO into $NiCl_2$ using chlorine at 600℃ was experimentally proven in previous works [15-16]. These results point out NiO as a corrosion reaction pathway, which is hard to accept considering high corrosion resistance of pure Ni against Cl_2 [11]. Further calculations were conducted using the HSC chemistry software, and the results are shown in Fig. 6. The ratio of chloride/oxide was calculated from the equilibrium composition of each metal as a function of Cl_2-O_2 input amount. Overall, it is clear that Ni has high chloride/oxide in the entire range except for the 0.2 mol Cl_2 + 0.2 mol O_2 case. It was identified that $FeCl_2$ was the only chloride in equilibrium and that is why there are no data for

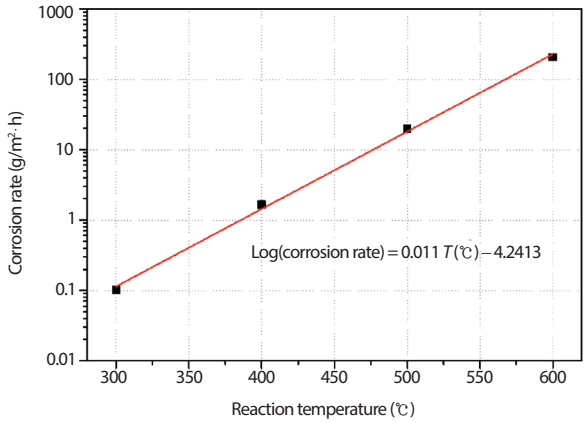

Fig. 7. The effect of the reaction temperature on the corrosion rate. The experiments lasted 8 h with flow rates of 170 mL/min for Ar and 30 mL/min for Cl_2.

Ni and Cr at this condition. When it comes to 0.6 mol Cl_2 + 0.6 mol O_2 case, the major chloride of Fe is changed from $FeCl_2$ to $FeCl_3$. The lowest chloride/oxide ratio of Cr in the entire range of calculation is in line with the high Cr/Ni ratio measured in the pits. According to the above calculation results, it can be concluded that the combination of Fe at low chlorine and oxygen partial pressure and Ni at relatively high chlorine and oxygen partial pressure contributed to the formation of pits in the Cl_2-O_2 mixed conditions.

The effects of the reaction temperature were investigated by means of experiments at temperatures of 300, 400, 500, and 600℃ with a chlorine flow rate of 30 mL/min (with an Ar flow rate of 170 mL/min). The results are summarized in Fig. 7 in the form of corrosion rate. A linear relationship was observed in the reaction temperature – corrosion rate (in logarithm scale) graph as shown in the figure meaning that a slight increase in the reaction temperature will lead to severe corrosion in the temperature range of this work. As there are no certain values of corrosion rate that decide applicability of a material, it is hard to define a certain temperature that SS-316 can be employed in the carbon anode OR equipment. However, these results can provide a scientific basis for material selection during a design of carbon anode OR equipment.

4. Conclusion

It was identified in this work that the presence of oxygen suppressed the corrosion of SS-316 by chlorine gas, while a linear relationship was observed between reaction time and weight loss regardless of gas composition. The results of a surface observation showed that the mixed gas condition produced an uneven surface with circular pits, which had a relatively Ni-poor composition. The thermodynamic investigations proposed the combination of $FeCl_2$ and $NiCl_2$ formation reactions as the reason of pit formation. The reaction temperature experiments showed that an increase in reaction temperature leads to an exponential increase in the corrosion rate.

Acknowledgements

This work was sponsored by the Nuclear R&D program of the Korean Ministry of Science and ICT (2017M2A85015077).

REFERENCES

[1] M.J. Song, “Korean Status and Prospects for Radioactive Waste Management”, J. Nucl. Fuel Cycle Waste Technol., 1(1), 1-7 (2013).

[2] G.-I. Park, M.K. Jeon, J.-H. Choi, K.-R. Lee, S.Y. Han, I.T. Kim, Y.-Z. Cho, and H.-S. Park, “Recent progress in waste treatment technology for pyroprocessing at KAERI”, J. Nucl. Fuel Cycle Waste Technol., 17(3), 279-298 (2019).

[3] C.E. Stevenson, The EBR-II fuel cycle story, American Nuclear Society, La Grange Park, Illinois (1987).

[4] Y. Sakamura and T. Omori, “Electrolytic reduction and electrorefining of uranium to develop pyrochemical reprocessing of oxide fuels”, Nucl. Technol., 171(3), 266-275 (2010).

[5] S.D. Herrmann, S.X. Li, M.F. Simpson, and S. Phongi-

karoon, “Electrolytic reduction of spent nuclear oxide fuel as part of an integral process to separate and recover actinides from fission products”, Sep. Sci. Technol., 41(10), 1965-1983 (2006).

[6] W. Park, E.Y. Choi, S.W. Kim, S.C. Jeon, Y.H. Cho, and J.M. Hur, “Electrolytic reduction of a simulated oxide spent fuel and the fates of representative elements in a Li_2O-LiCl molten salt”, J. Nucl. Mater., 477, 59-66 (2016).

[7] E.Y. Choi, J. Lee, D.H. Heo, S.K. Lee, M.K. Jeon, S.S. Hong, S.W. Kim, H.W. Kang, S.C. Jeon, and J.M. Hur, “Electrolytic reduction runs of 0.6 kg scale-simulated oxide fuel in a Li_2O-LiCl molten salt using metal anode shrouds”, J. Nucl. Mater., 489, 1-8 (2017).

[8] A. Merwin, P. Motsegood, J. Willit, and M.A. Williamson, “A parametric study of operating carbon anodes in the oxide reduction process”, J. Nucl. Mater., 511, 297-303 (2018).

[9] S.W. Kim, M.K. Jeon, H.W. Kang, S.K. Lee, E.Y. Choi, W. Park, S.S. Hong, S.C. Oh, and J.M. Hur, “Carbon anode with repeatable use of LiCl molten salt for electrolytic reduction in pyroprocessing”, J. Radioanal. Nucl. Chem., 310(1), 463-467 (2016).

[10] S.W. Kim, D.H. Heo, S.K. Lee, M.K. Jeon, W. Park, J.M. Hur, S.S. Hong, S.C. Oh, and E.Y. Choi, “A preliminary study of pilot-scale electrolytic reduction of UO_2 using a graphite anode”, Nucl. Eng. Technol., 49(7), 1451-1456 (2017).

[11] M.H. Brown, W.B. Delong, and J.R. Auld, “Corrosion by chlorine and by hydrogen chloride at high temperatures”, Ind. Eng. Chem., 39(7), 839-844 (1947).

[12] Y. Ihara, H. Ohgame, K. Sakiyama, and K. Hashimoto, “The corrosion behaviour of iron in hydrogen chloride gas and gas mixtures of hydrogen chloride and oxygen at high temperatures”, Corros. Sci., 21(12), 805-817 (1981).

[13] HSC Chemistry software, Outotec, Pori, Finland.

[14] F.J. Alvarez, D.M. Pasquevich, and A.E. Bohe, “Kinetics of the recovery of nickel from depleted catalysts used in the reforming of methane”, Int. J. Hydrogen Energy, 33(13), 3438-3441 (2008).

[15] I. Ilic, B. Krstev, K. Cerovic, and S. Stopic, “The study of chlorination of nickel oxide by chlorine and calcium chloride in the presence of active additives”, Scand. J. Metall., 26(1), 14-19 (1997).

[16] T.A. Anufrieva, L.E. Derlvukova, and M.V. Vinokurova, “Interaction of nickel oxide with chlorine”, Russ. J. Inorg. Chem., 46(1), 16-19 (2001).